Electronic Supplementary Material (ESI) for New Journal of Chemistry.

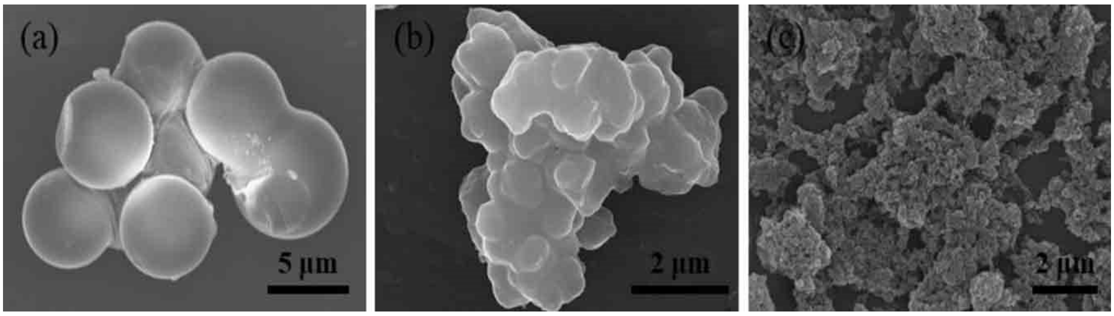

Fig. S1 SEM of NCA-1(a)、NCA-2(b)、NCA-3(c)

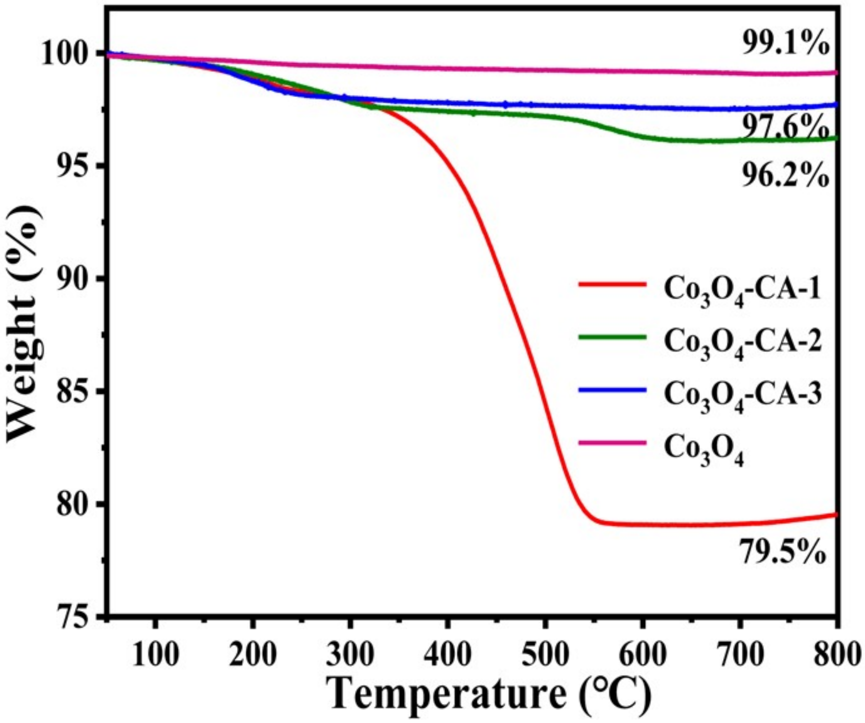

Fig. S2 TG analysis of Co_3O_4@NCA-1, Co_3O_4@NCA-2, Co_3O_4@NCA-3 and Co_3O_4 materials.

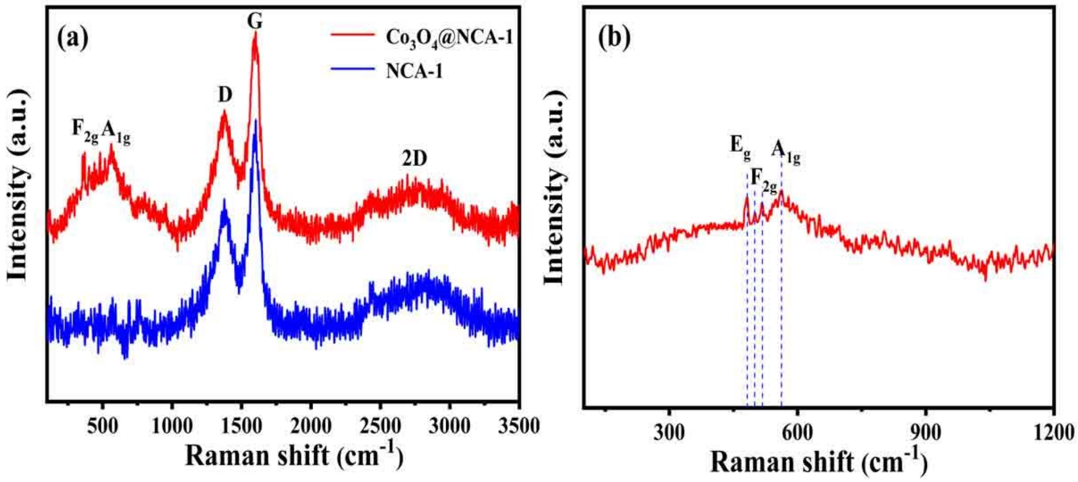

Fig. S3 Raman of NCA-1 and Co_3O_4@NCA-1(a) and partial enlarged detail of Co_3O_4@NCA-1 (b).

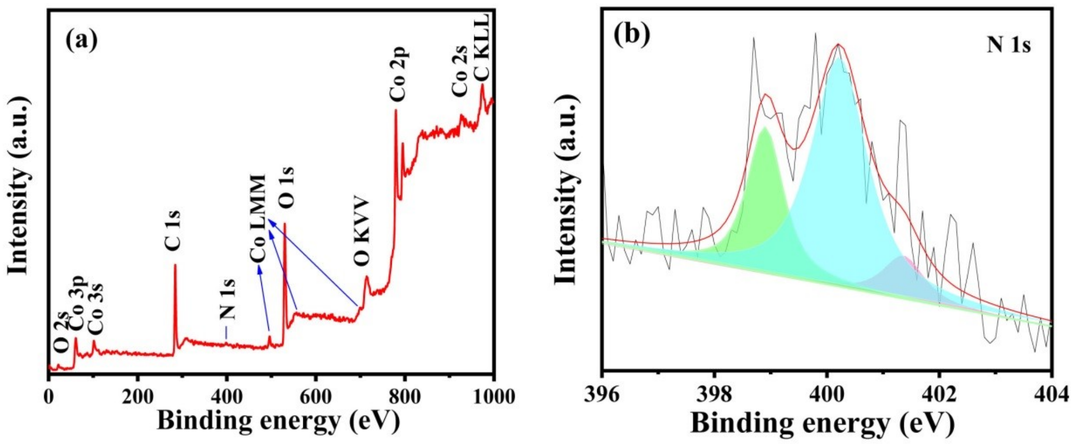

Fig. S4 XPS full spectra of Co_3O_4@NCA-1 (a) and N1s spectra of Co_3O_4 coated with high content of NCA-1(b).

.

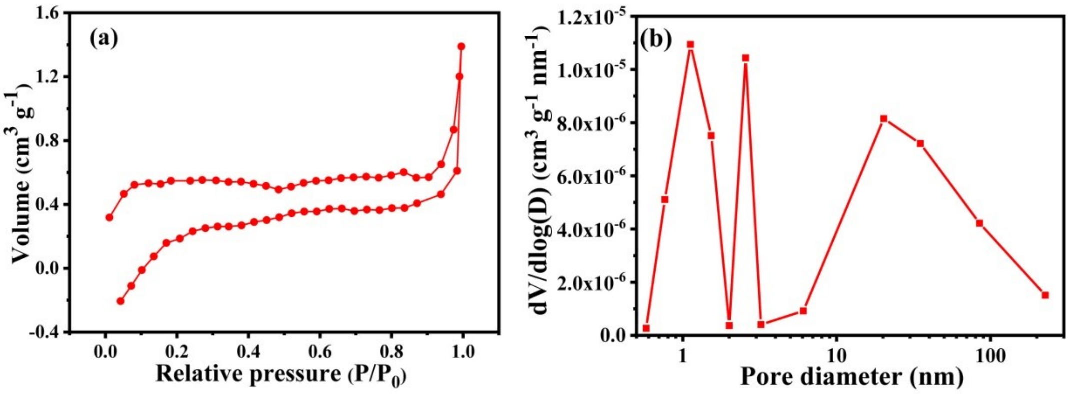

Fig. S5 Nitrogen adsorption-desorption isotherms (a) and BJH pore diameter distribution curve (b) of NCA-1.

The specific surface area of NCA-1 is 2.8 m²/g, which is lower than that of Co_3O_4 (5.3 m^2 g^{-1}) and ever lower that of Co_3O_4/NCA-1(355.5 m^2 g^{-1}). It exhibits a type IV isotherm shown in Fig. 2(a), similar to Co_3O_4 and Co_3O_4@NCA-1. Furthermore, the pore size distribution demonstrated that not only mesopores and macropores but also micropores are present in the NCA-1 material, which would contribute to lithium storage performance.

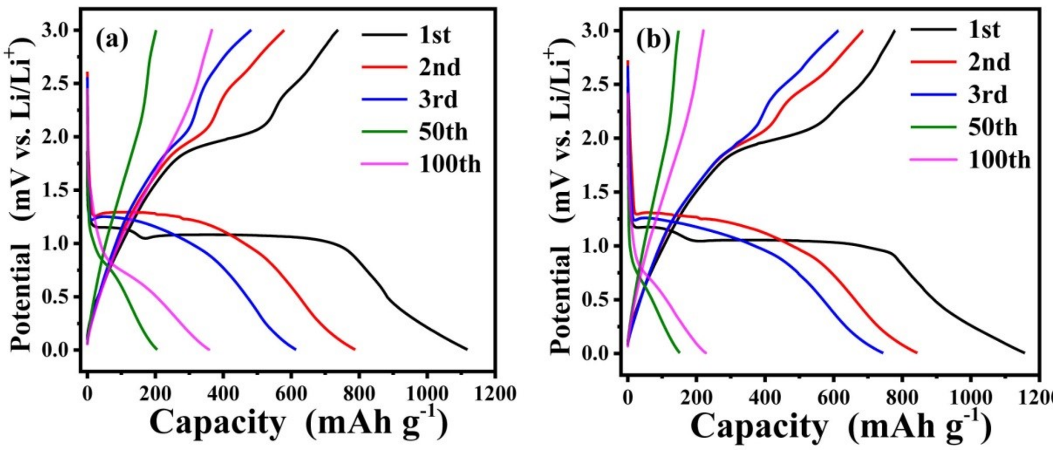

Fig. S6 The initial three, the 50th and the 100th CV curves of Co_3O_4@NCA-2(a) and Co_3O_4@NCA-3(b).

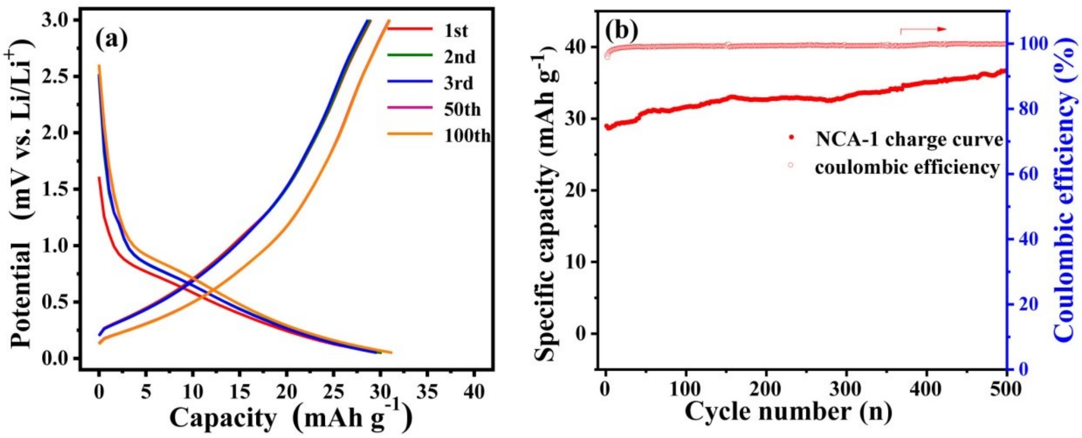

Fig. S 7 The charge/discharge curves (a) and cycling performance (b) of NCA-1 at a current density of 0.1A g^{-1}.

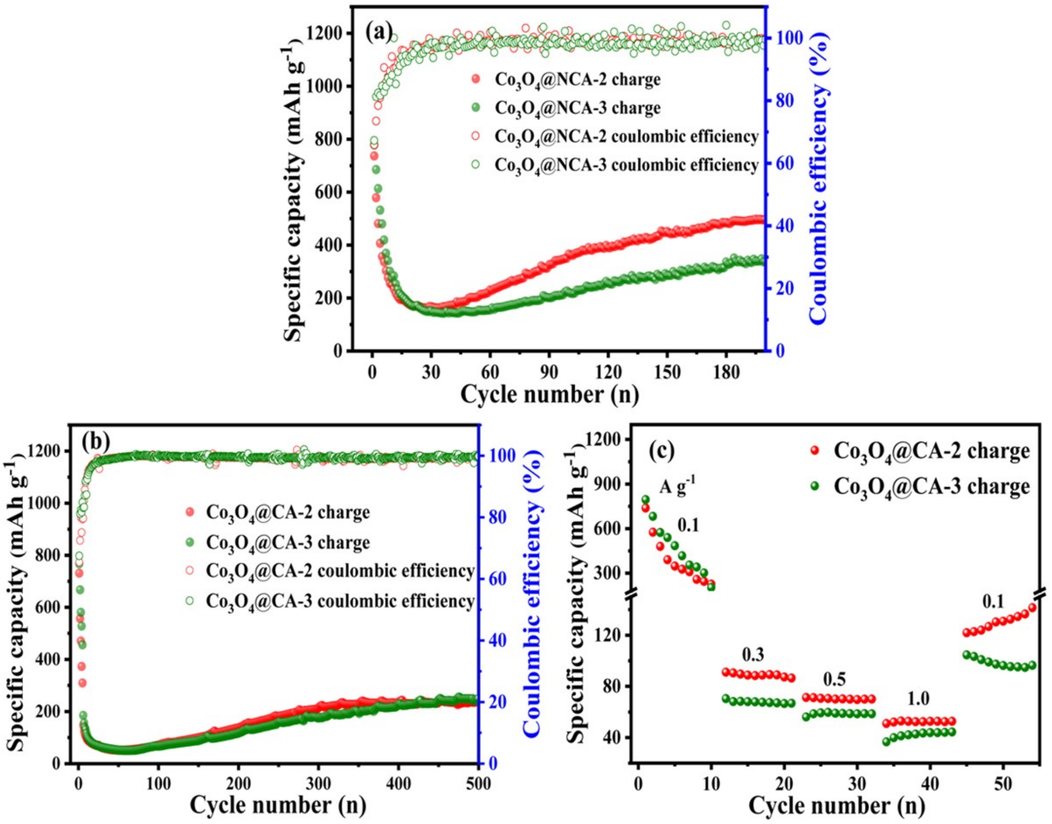

Fig. S8 Cycling performance and the corresponding coulombic efficiency of Co_3O_4@NCA-2 and Co_3O_4 @NCA-3 at 0.1 A g^{-1} (a) and 0.5 A g^{-1} (b), rate performance of Co_3O_4@NCA-2 and Co_3O_4 @NCA-3(c).

Tab. S1 Comparison of the electrochemical performances of various cobalt-based/carbon nanocomposites as anode materials for LIBs

Active material	Current density mA g^{-1}	Capacity mAh g^{-1} (Nth)	Reference
Co_3O_4 @NCA-1	100	608(200)	This work
	100	659.9(100)	
	500	291.7(500)	
NiO-Co_3O_4	70	673 (100)	[44]
Co_3O_4	89	423(30)	[45]
	89	321(60)	
Co_3O_4@TiO_2@C	200	380.3(100)	[46]
Co_3O_4	90	166(100)	[47]
Co_3O_4/TiO_2	100	660(120)	[48]